Upgrading the Near Detector of T2K, the Beam Test of a New Scintillator Detector Design, and Electron Neutrino Detection in a Neutrino Beam

Wilf Shorrock

Imperial College London
(Dated: July 2, 2018)

In 2020, the Tokai-to-Kamioka (T2K) experiment is set to enter a new phase of data-taking with a more intense neutrino beam. To make full use of the higher statistics and reduce systematic errors, upgrades to the one of the near detectors—ND280—have been proposed. In this report, the physics of neutrino oscillations are explained and an outline of the T2K experiment is given. The sub-detectors currently comprising ND280 and the structure of its software is described, as well as proposed upgrades. A beam test performed at CERN in June 2018 for the prototype of the new Super-fine-grained detector (Super-FGD), to be installed in the upgraded ND280, is also detailed. A rough plan of the future work the author will undertake is given at the end of the report, which includes analysis of ND280 data for electron neutrino and anti-electron neutrino interactions in the neutrino beam.

CONTENTS

I. INTRODUCTION

The imprint neutrinos leave on our world is almost unnoticeable due to their vanishingly small cross-sections with respect to everyday baryonic matter. Yet, the ethereal nature of the neutrino belies its importance in the Universe. Neutrinos have pervaded our world almost since the very beginning and they have affected the evolution of entire galactic systems. This is why physicists are persevering in their attempts to measure the properties of the almost undetectable neutrino, a study in which they have made notable progress over the past few decades.

Since the neutrino was first discovered in 1956 by Reines and Cowan [1], the way in which it has been perceived by the scientific community has evolved significantly. After initially thinking all neutrinos were identical, we now know they come in three different flavours: electron, muon and tau neutrinos. Each flavour contributes a lepton number of +1 or -1 for its corresponding lepton flavour in all the interactions they participate in, albeit they are extremely rare interactions. The notion of neutrinos having mass is also a new concept, with the neutrino thought of as massless before it was discovered that neutrinos could oscillate in flavour, which is partly credited to the flavour change in atmospheric neutrinos observed by the Super-Kamiokande (SK) water Cherenkov detector in the 1990s [2]. This effect implies that neutrinos must have some mass, although to have been unmeasured thus far it has to be extremely small, as explained in Sec. II of this report.

There are several experiments measuring oscillation parameters using neutrinos produced in nuclear reactors, such as KamLAND, Daya Bay, and Double CHOOZ [3–5]. There are also experiments using neutrino beams produced using particle accelerators. The goals of these latter experiments are to make more precise measurements of the oscillation parameters and to ascertain whether charge parity (CP) is conserved or not.

Tokai to Kamioka (T2K) is an experiment that measures neutrino oscillations over a long distance. It studies neutrinos produced by a proton accelerator. Since it began taking data in 2010, T2K has made precision measurements of the neutrino squared mass splittings and several mixing angles, including one of the first measurements of the mixing angle θ_{13} (these parameters are explained in Sec. II) [6]. The latest analysis results were published in 2017 [7]. Over the next few years, the experiment aims to observe CP violation (CPV) in neutrino oscillations with at least a 3σ statistical significance (if the CPV is maximal) and discover whether the mixing angle θ_{23} is maximal, as current measurements suggest. The new phase of the experiment is called T2K-II and will require several upgrades to the experiment's detectors.

This paper provides an overview of the proposed upgrades to the T2K experiment's off-axis near detector, ND280. It also gives a description of the beam test carried out with the prototype of one of the new sub-detectors, called the Super-FGD. This description will include a calibration measurement for the detector's photosensors and initial data readings from the beam test. The final section of the report will address my future work, such as the continued development of the ND280 software and an analysis of ND280 data using a new neutrino generator production. Firstly, the theory behind neutrino oscillation will be given, leading on to an overview of the T2K experiment and details on the current state of ND280 and its software.

II. NEUTRINO OSCILLATION MODEL

For neutrino oscillations to exist, the neutrino flavour eigenstates, $(\nu_e, \nu_\mu, \nu_\tau)$, must be different to the neutrino mass eigenstates, (ν_1, ν_2, ν_3). In fact, it must be the case that the flavour eigenstates are coherent superpositions of the mass eigenstates. Hence, they can be equated using the equation

$$\begin{pmatrix} \nu_e \\ \nu_\mu \\ \nu_\tau \end{pmatrix} = \begin{bmatrix} U_{e1} & U_{e2} & U_{e3} \\ U_{\mu 1} & U_{\mu 2} & U_{\mu 3} \\ U_{\tau 1} & U_{\tau 2} & U_{\tau 3} \end{bmatrix} \begin{pmatrix} \nu_1 \\ \nu_2 \\ \nu_3 \end{pmatrix}, \tag{1}$$

where the matrix enclosed by square brackets is the Pontecorvo-Maki-Nakagawa-Sakata (PMNS) matrix, $\boldsymbol{U}$ [8, 9]. The matrix elements $U_{\alpha i}$ represent the mixing amplitudes of mass state i contained within flavour state ν_α.

$\boldsymbol{U}$ is a unitary matrix, so it can be parametrised using three real angles, $(\theta_{12}, \theta_{13}, \theta_{23})$, and a real phase, δ_{CP}, to give

$$\boldsymbol{U} = \begin{bmatrix} 1 & 0 & 0 \\ 0 & C_{23} & S_{23} \\ 0 & -S_{23} & C_{23} \end{bmatrix} \begin{bmatrix} C_{13} & 0 & S_{13}e^{-i\delta_{\mathrm{CP}}} \\ 0 & 1 & 0 \\ -S_{13}e^{i\delta_{\mathrm{CP}}} & 0 & C_{13} \end{bmatrix} \begin{bmatrix} C_{12} & S_{12} & 0 \\ -S_{12} & C_{12} & 0 \\ 0 & 0 & 1 \end{bmatrix}, \tag{2}$$

where $C_{ij} = \cos\theta_{ij}$ and $S_{ij} = \sin\theta_{ij}$. These mixing angles and phases are what oscillation experiments measure. A non-zero value of the δ_{CP} phase (given that $S_{13} \neq 0$) would mean that neutrino oscillations are CP-violating. There may be two extra phase parameters required if neutrinos are Majorana particles (Majorana particles are their own anti-particles) but these have no effect on oscillation measurements [10].

Eq. (1) encapsulates much of the physics behind neutrino oscillations. It implies that, following the weak decay $W \to l_\alpha \nu_\alpha$, where ν_α is a neutrino flavour eigenstate and l_α is the corresponding charged lepton state with flavour α, the neutrino will propagate as a mixture of the mass eigenstates that interfere quantum mechanically in interactions. This means the probability of the neutrino's flavour, when measured, is dependent on the distance the neutrino travelled [10].

For a detailed derivation of the neutrino oscillation probabilities, see Kayser [11]. Here, we will quote the end result only, which is the probability of a (anti-)neutrino with initial flavour α and energy E_ν propagating a distance L and being detected with flavour β:

$$\begin{aligned} P\left(\overset{(-)}{\nu}_\alpha \to \overset{(-)}{\nu}_\beta\right) = \delta_{\alpha\beta} &- 4\sum_{i<j}^{3} \Re[U_{\alpha i}U^*_{\beta i}U^*_{\alpha j}U_{\beta j}] \sin^2\left(\Delta m^2_{ij}\frac{L}{4E_\nu}\right) \\ &\mp 2\sum_{i<j}^{3} \Im[U_{\alpha i}U^*_{\beta i}U^*_{\alpha j}U_{\beta j}] \sin\left(\Delta m^2_{ij}\frac{L}{2E_\nu}\right), \end{aligned} \tag{3}$$

where $\Delta m^2_{ij} = m^2_i - m^2_j$ is the difference between the squared masses of mass eigenstates i and j. Δm^2_{ij} is another set of parameters that oscillation experiments measure, in lieu of the absolute masses of each neutrino flavour, which are as yet unmeasured.

Eq. (3) can only be applied to neutrinos travelling through a vacuum. For neutrino propagation through matter, see the report by Kayser [10].

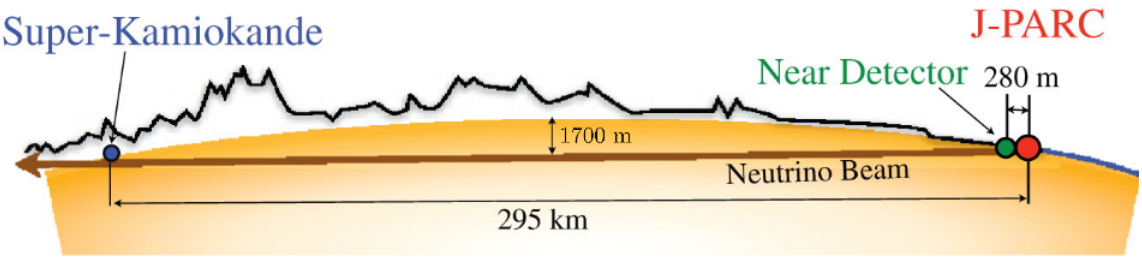

FIG. 1: The path of the neutrino beam produced in the T2K experiment [12].

III. T2K

The T2K experiment spans 295 km from the east coast of the largest Japanese island, Honshu, to the west coast. The size of the experiment is one of its assets, as it gives access to areas of the oscillation parameter space that shorter baseline experiments can't sample.

The neutrino beam of T2K is generated at the Japan Proton Accelerator Research Complex (J-PARC) in Tokai. Protons from the accelerator collide with a graphite target and produce charged pions that are focused into a beam. These pions then decay to give muons and muon neutrinos. The muons, and mesons that have not yet decayed, are stopped by a beam dump, which just leaves the muon neutrinos. These neutrinos travel through the Earth towards the other end of the experiment in Kamioka.

In Tokai, the neutrino beam passes through two near detectors—INGRID and ND280—that are 280 m from the graphite target. At the other end of the experiment, in Kamioka, the far detector—SK—observes interactions from neutrinos in the beam. An illustration of the experiment is shown in Fig. 1.

The INGRID detector lies on the axis of the neutrino beam, but ND280 and SK are 2.5° off-axis, which sets the peak of the neutrino flux at 600 MeV, the energy at which muon neutrino disappearance is most likely using current oscillation parameter values.

The content of the neutrino beam used in T2K can be switched between muon neutrinos (ν_μ) and anti-muon neutrinos ($\bar{\nu}_\mu$). The pions produced in the collisions between the protons and the graphite target are focused by electromagnetic horns. Reversing the current passed through the horns causes particles of opposite charge to be focused and the opposite charge to be deflected, hence one can focus positive pions (π^+) or negative pions (π^-) depending on the current's direction. The mode in which π^+s are focused to give a ν_μ beam is the forward horn current (FHC) mode. To focus π^-s and create a $\bar{\nu}_\mu$ beam the reverse horn current (RHC) mode is needed.

In the next section, details on T2K's ND280 detector and its proposed upgrades for the next phase of data-taking are given. Information on the other T2K detectors and the beamline is given elsewhere [12].

IV. ND280: CURRENT STATE

ND280 gathers data on the neutrino beam to estimate the beam's flux, energy spectrum, and flavour content. This allows comparison with measurements at the far detector, leading to calculations of neutrino oscillation parameters by observing how the flavour content of the beam has changed as a function of energy.

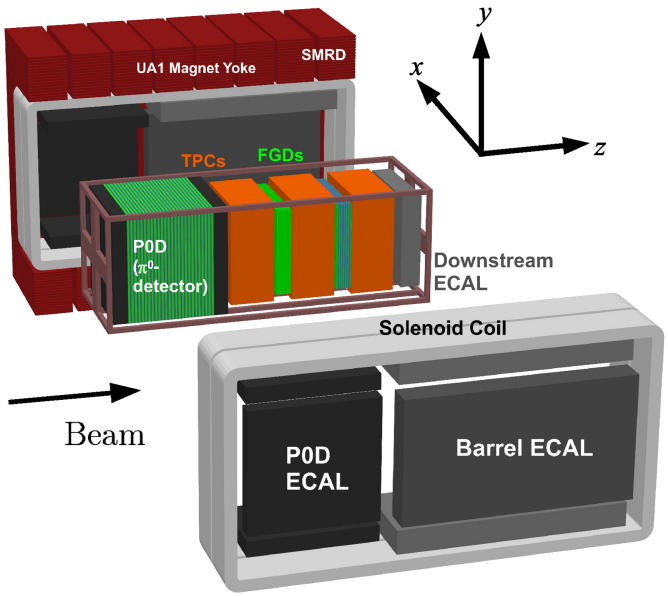

FIG. 2: Expanded view of the ND280 detector, showing the positions of each of the three main sub-systems and sub-detectors. The entire detector is encased in the UA1 magnet with a 0.2 T magnetic field [12].

As well as monitoring the beam characteristics, ND280 also takes data for neutrino cross-section measurements, providing the community of neutrino oscillation experiments with data to evaluate their interaction models.

The detector can be broken down into three sub-detectors: a π^0 detector (PØD), a tracker consisting of two fine grain detectors (FGDs) and three time-projection chambers (TPCs), a system of electromagnetic calorimeters (ECals), and a side muon range detector (SMRD). The whole detector is subject to a 0.2 T magnetic field for charge identification and momentum determination. See Fig. 2 for a visualisation of the ND280 detector, its sub-detectors, and the xyz axes used to describe detector orientations in the rest of this section.

The sub-detectors of ND280 will now be described in more detail, apart from the SMRD, as it is not relevant to this work. Instead, it can be read about in the literature [13]. An introduction to the software used by ND280 will also be given.

A. π^0 Detector (PØD)

T2K's far detector, SK, has difficulty discerning between electrons and the double gamma signal produced in neutral pion (π^0) decay. To reduce this systematic error, the PØD sub-detector of ND280 is used to measure the cross-sections of neutrino interactions, specifically with water, where a π^0 appears in the final state. Using this cross-section data, the number of π^0s produced in SK can then be calculated and taken into account.

The central section of the PØD consists of alternating layers of brass, plastic scintillator, and fillable water bags. The brass acts as a radiator whereas the water and plastic layers provide a target for neutrinos to interact with. Plastic scintillator has the useful property of emitting photons when a charged particle passes through it. This is exploited by using wavelength shifting (WLS) fibres to read off the light signal from a passing particle and

using the data to reconstruct the particle's trajectory.

The central target is preceded and followed by electromagnetic calorimeters comprised of alternating sheets of lead and scintillator. These ECals are used for rejecting particles entering the PØD that originated from outside the detector and also to contain and measure electromagnetic showers.

Cross-section values with respect to the water target can be deduced by taking measurements when the target bags in the central section are filled with water and comparing them to when they filled with air [12, 14].

B. Fine Grain Detectors (FGDs)

The FGDs provide 2.2 tonnes of mass with which incoming neutrinos can interact and precision tracking to map out the interaction vertices. They consist of bars of plastic scintillator oriented perpendicular to the neutrino beam and stacked side-to-side to form sheets. Two sheets are placed one after the other to form a module, with the bars of one layer being arranged vertically (along the y-axis) and the other layer horizontally (along the x-axis). The bars are read-off by WLS fibres, so the position of a charged particle incident on a module can be determined in two dimensions. Placing several modules in sequence then gives the trajectory of a particle through the detector

There are two FGDs in ND280. The downstream FGD also contains layers of water in between the scintillator layers. Comparing interaction rates between the two FGDs allows calculation of the cross-sections of neutrino interactions with carbon and water [12, 15].

C. Time Projection Chambers (TPCs)

There are three TPCs in ND280, sandwiching the two FGDs. The bulk of each TPC consists of 3000 litres of an argon-based gas. When charged particles pass through this gas, they ionise the gas molecules. The ionisation electrons drift away from a cathode and towards a readout plane. The location and arrival time of the electrons on this plane can be used to construct a 3D image of the particle's trajectory.

TPCs are ideal for identifying the number and trajectory of charged particles in the detector, although their relatively small mass makes it unlikely for a neutrino to interact with them, hence the need for FGDs. The information provided by TPCs allows selection of low-contamination interaction samples, as well as momentum measurements from curved tracks caused by the magnetic field present in the detector. Combining a particle's momentum along with the ionisation of the particle's track, one can identify the type of particle that made the track. Hence, when combined with the FGD data, the TPCs can be used to help identify neutrino interactions in ND280 and to determine the electron neutrino contamination in the muon neutrino beam [12, 16].

D. Electronic Calorimeter (ECal)

As well as the ECals either end of the PØD, there are also ECals surrounding the entire detector. A "barrel" ECal encompasses the tracker around the z-axis, another ECal is situated downstream of the tracker, and a third encircles the PØD about the z-axis.

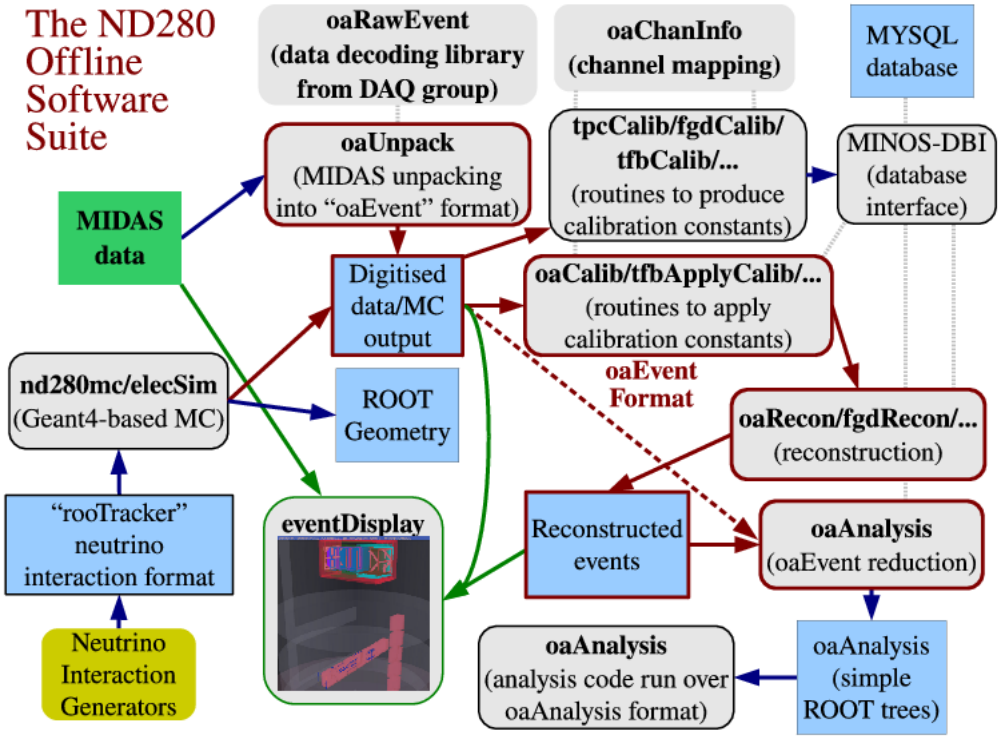

FIG. 3: The flow of data through the package structure of the ND280 software. The flow is simplified and only shows the most relevant packages. Boxes with red coloured borders represent packages that process oaEvent data. [12]

The main uses of the ECals are to complement the inner detectors by measuring the energies of photons missed by the inner detectors, reject particles from interactions outside the detector, and help with particle identification.

Alternating layers of scintillator and lead absorber make up each ECal. The scintillator layers consist of several bars of plastic scintillator. These bars are oriented perpendicular to the scintillator bars of the adjacent layers, similar to the FGDs [12].

E. ND280 Software

The ND280 software is used for offline analysis of data collected by ND280, as well as Monte Carlo (MC) data generation and analysis. The basic framework of the code was built in 2004, with the underlying structure and data storage relying on ROOT [17], simulation libraries from Geant4 [18], a package management system provided by CMT (Configuration Management Tool) [19] and the version control system used to store each version of the code is CVS (Concurrent Version Systems) [20].

A decision was made early-on in the software's lifetime to split the structure of the software into different packages, resulting in about 60 software packages in total [12]. This offers easy access to specific areas of code and makes editing the software simpler for developers.

The flow-path of the different data types through the package structure is shown in Fig. 3, but only the most relevant packages are shown.

The package oaEvent (the "oa" prefix stands for "off-axis") is important as it defines the format of the data passed through the software between the steps where raw MIDAS data

(MIDAS is the format of data from the ND280 detector [21]) is passed to the software and the final step where oaAnalysis reduces the data to a user-friendly format. The oaUnpack and oaRawEvent packages handle the conversion of MIDAS data to oaEvent data. oaCalib then applies calibration constants to the data, whilst oaCalib's sub-packages use the data to produce calibration constants to store in MYSQL, which are used by oaCalib. The data is then passed on to oaRecon, which uses the data to reconstruct the particle events that occurred in the detector, the results of which are analysed by oaAnalysis.

The exact same processes are applied to MC generator data, except that the data does not start in MIDAS format. The MC data is produced by passing information from the neutrino flux packages to the neutrino interaction generators NEUT [22] and GENIE [23]. These generators produce realistic distributions of child particles from neutrino interactions. The simulation is then taken over by nd280mc, which uses Geant4 to propagate the child particles and simulate the energy deposits left in the detector. elecSim then converts these energy deposits to simulated electrical readouts, as would be seen in the real detector and recorded in MIDAS format, except here it is written as oaEvent data.

V. HARDWARE UPGRADES

Resulting from T2K's success in measuring oscillation parameters with improved precision, the experiment is set for a series of upgrades to further increase the measurement precision. In tandem with these improvements, ND280 must also be revamped to reduce systematic uncertainties in the neutrino appearance predictions and cross-section measurements. Here, we will go through the proposed upgrades that are planned for construction over 2019–2020 to be installed in Japan by 2020 [24].

A. Scintillator Detector and Horizontal TPCs

The proposed upgraded ND280 is shown in Fig. 4. The downstream end of the detector will remain unchanged, with three TPCs separated by two FGDs followed by an ECal. At the upstream end, however, the central PØD module (not the ECal endcaps) will be replaced by a scintillator detector sandwiched between two horizontal TPCs. The reason for the PØD's removal is the large value of θ_{13}, making it's measurements to estimate the double gamma backgrounds at SK less necessary than previously thought, as the background is significantly smaller than the observed signal.

The scintillator detector will act as a target material, with the TPCs distributed around it giving nearly 4π solid angle coverage. This will address an issue with the old ND280 design: the tracking efficiency is biased towards low scattering angles. This is because, after a neutrino has interacted in an FGD, the resulting lepton is only seen clearly in the downstream TPC if the scattering angle is less than about 40° with respect to the beam direction. The TPC gives important information on the interaction, so most interaction samples exclude leptons with high scattering angles. This creates problems when comparing data with SK, which has a flat efficiency with respect to scattering angle.

The new scintillator detector will have a first-of-its-kind "Super-FGD" design that incorporates scintillator cubes rather than bars, which can be read out from three orthogonal directions by WLS fibres. The cubes' side length will be between 1–2 cm, with the larger lengths sacrificing granularity for a smaller number of cubes and readouts. The size of the

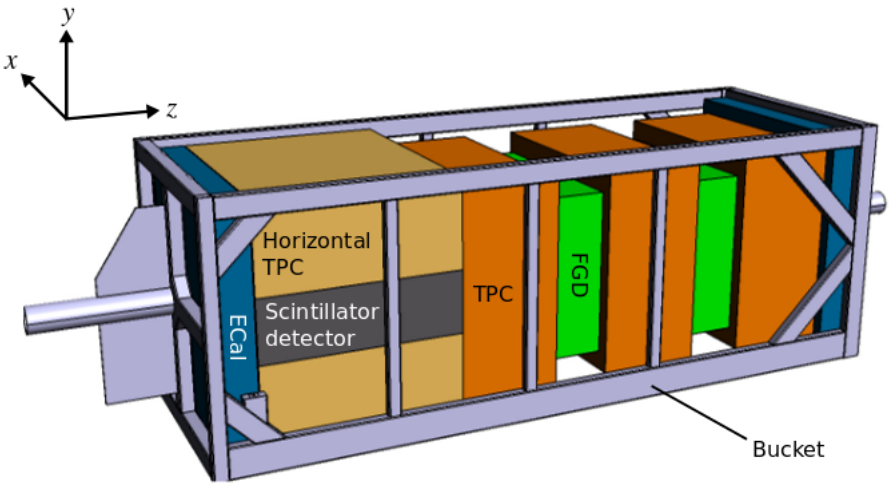

FIG. 4: The proposed upgrade of ND280. The new additions are the horizontal TPCs and the scintillator detector, which replace the PØD. The "bucket" is a framework that supports the detectors. Not shown are the barrel ECals that will surround the detectors, similar to the original design. The neutrino beam propagates in the z direction [24].

cubes is comparable to the height and width of the scintillator bars used in the current design, but the bars only give readouts in two directions. The extra information provided by the cubes helps to reconstruct the paths of multiple particles. This means it will be easier to discern electrons produced from neutrino interactions from electron-positron pairs produced by gamma particles. It will also give larger data samples of multi-nucleon final state interactions, which are one of the main contributors to systematic errors in analyses. Fig. 5 shows an illustration of the Super-FGD design.

Prototypes of the horizontal TPC and the Super-FGD will be used in test-beams at CERN, the latter of which is being tested at the time of this report being submitted. Details of the Super-FGD's beam test will be given in Sec. VI.

B. Time of Flight Detectors

Not shown in the diagram of the ND280 upgrade (Fig. 4) are the new time-of-flight (TOF) detectors that are to be installed. These will be placed around the volume containing the scintillator detector and the horizontal TPCs. The TOF detectors will help identify whether a particle originated from inside or outside the detector and will also aid with particle identification. The design of the TOF detectors is as yet undecided. There are two possible candidates, one based on wavelength shifting fibres and the other based on plastic scintillator bars. A prototype of the latter design is being constructed in 2018 and will be tested later in 2018 [24].

VI. SUPER-FGD BEAM TEST

The beam test for the Super-FGD prototype is scheduled for June 27th – July 11th 2018, taking place at CERN using the T9 beam line.

The main goals of the beam test are:

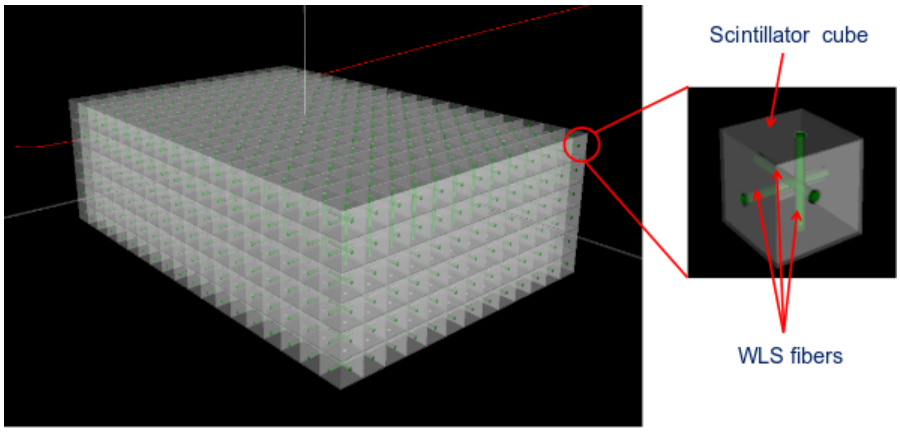

FIG. 5: A rendering of the Super-FGD to be used in the upgraded ND280. The detector comprises many small plastic scintillator cubes that are read off in three orthogonal directions by wavelength shifting fibres. There are fewer cubes depicted here than there will be in the actual detector, to make the diagram clearer [24].

- Illuminate the detector with roughly 5 GeV muons to ascertain the detector's properties such as time resolution, position resolution, pulse height uniformity, alignment and more. This will also provide an opportunity to calibrate the detector.
- Fire a beam of gamma particles at the detector to study the particle identification (PID) between electrons and gamma rays in the device and the two-track separation of electron-positron pairs.
- Use an uncollimated beam of hadrons and muons and measure energy loss of particles and study the effects of particles stopping in the detector.
- Collect samples of low energy protons from elastic scattering events with pions ($\pi^+ p \rightarrow \pi^+ p$).
- Observe high energy pion interactions that produce many particles to test multi-track separation.

The results of the beam test will be known after July 11th 2018. The prototype's design, the set-up of the beam test, and the method of photosensor calibration are reported here. Some preliminary data taken on the beam line is also shown.

A. The Super-FGD Prototype

The prototype scintillator detector measures $24 \times 48 \times 8$ cm^3 (the actual Super-FGD will be over 200 times larger) and comprises 9216 extruded cubes of polystyrene mixed with p-terphenyl plastic scintillator, each 1 cm long. There are a total of 1728 WLS fibres threaded through the cubes. On one end of each fibre is a plastic connector. This attaches to another connector, which houses a multiple pixel photon counter (MPPC) that sends a signal down a length of cable to the data acquisition (DAQ) system (MPPCs will be explained later in Sec. VI C). Two photographs of the prototype are shown in Fig. 6. Fig. 6a shows the construct as a whole, housed in its frame. The frame is used to attach the detector to a sliding platform

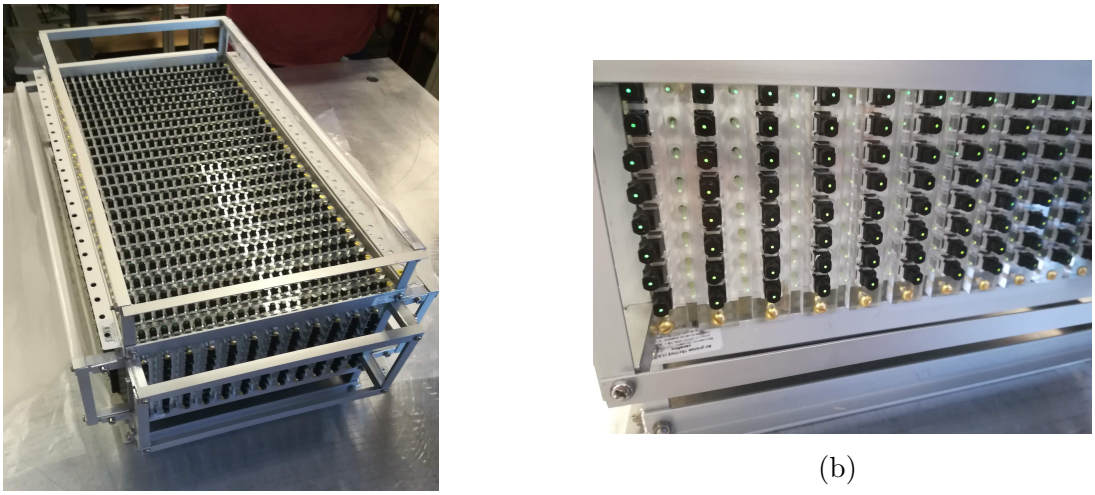

(a) (b)

FIG. 6: Photographs of the Super-FGD prototype after being delivered to CERN. These were taken before the electronics were fitted for the beam test. (a) shows the whole detector, along with the frame it is housed in. (b) is a close-up of one of the detector's sides, giving a clear view of the scintillator cubes and the WLS fibres. The black connectors are where the readout electronics will be attached.

and the cables connecting the detector to the readout electronics can be tied to the sides of the frame. Fig. 6b displays a close-up of the side of the detector, giving a detailed view of the connectors at the ends of the WLS fibres, which will connect the detector to the DAQ system.

B. The Beam Test Configuration

The beam test is taking place in the East Area of the Proton Synchrotron at CERN. Test-beam T9 is being used to fire p, e^+, e^-, π^+, π^-, μ^+ and μ^- particles at the Super-FGD prototype with momenta ranging between roughly 0.5–5 GeV (this is the expected momentum range for particles to be produced in the ND280 detector) [25].

The prototype is placed inside the MNP17 magnet, which is present for PID [26]. The magnetic flux density is set to 0.2 T, the same as the UA1 magnet of ND280. All readout electronics need to be placed outside the magnet field, hence long cables (about 1.5 m long) are used to connect the detector to the electronics.

Fig. 7 shows how the detector is oriented with respect to the magnet, as well as the readout electronics, which are kept in metal boxes called "minicrates". The prototype is kept on a rotating platform so the detector's response to particles incoming at several angles can be tested.

The DAQ system in the minicrates is the same one that will be used for Baby MIND (Baby magnetised iron neutrino detector) [28]. This is used concurrently with another DAQ system using a WaveCatcher digitiser [29]. The system is connected to several hodoscopes and Cherenkov detectors, which will act as a trigger system and give PID. Baby MIND has its own trigger system, so its results will be compared with those of the WaveCatcher system, as a means of corroboration.

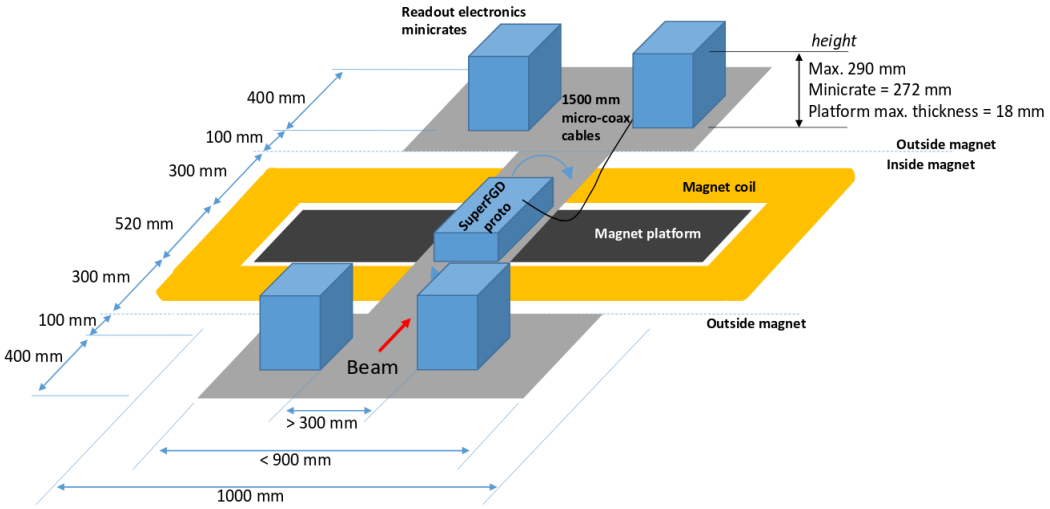

FIG. 7: A plan of the orientation of the prototype detector and its DAQ electronics with respect to the MNP17 magnet. Not shown is the upper platform of the magnet, which sits 290 mm above the lower platform. In order to access the prototype during the beam test, it is placed on a mechanical platform that can slide out of the magnet. The platform also rotatea about the horizontal axis parallel to the beam and the vertical axis to allow different orientations of the prototype with respect to the beam [27].

The layout of the detectors used in the trigger system is shown in Fig. 8. There are three hodoscopes in total, along with two Cherenkov detectors. By monitoring these detectors the trigger can be activated when a signal is produced in each one within a certain time window. Time of flight information can also be used to distinguish protons from lighter particles. The Cherenkov detectors help with PID by distinguishing electrons from muons and pions. In the 0.5–5 GeV momentum range only electrons produce Cherenkov light in these detectors, making it easy to identify them.

C. MPPC Calibration

MPPCs are silicon photomultipliers with a negative bias voltage just above the breakdown voltage of the silicon. An array of Geiger Mode Avalanche Photo-Diode pixels is present on each sensor. When a photon interacts with one of the pixels, a photoelectron is produced. The photoelectron is then accelerated by the bias voltage, creating electron-hole pairs in the silicon as it travels. This results in the initial charge created by the photon to increase significantly, like a snowball turning into an avalanche (hence the naming of the pixels). For the Super-FGD prototype, the charge from the MPPCs is sent to a front-end board and integrated. This integrated charge is then converted into a signal count using an analog-to-digital converter (ADC). The massive gain in charge means the signal produced is larger than background readings, allowing the detection of single photons. In fact, a single photon can saturate a pixel, which is why multiple pixels are used.

The signal from an MPPC has a distinctive spiky profile, with each spike corresponding to a burst of charge from a photon, or several photons at once. Fig. 9 shows an example of the signal from an MPPC. The first peak in the plot corresponds to the ADC counts produced by a single photon, the second peak corresponds to the ADC counts of two photons, and so

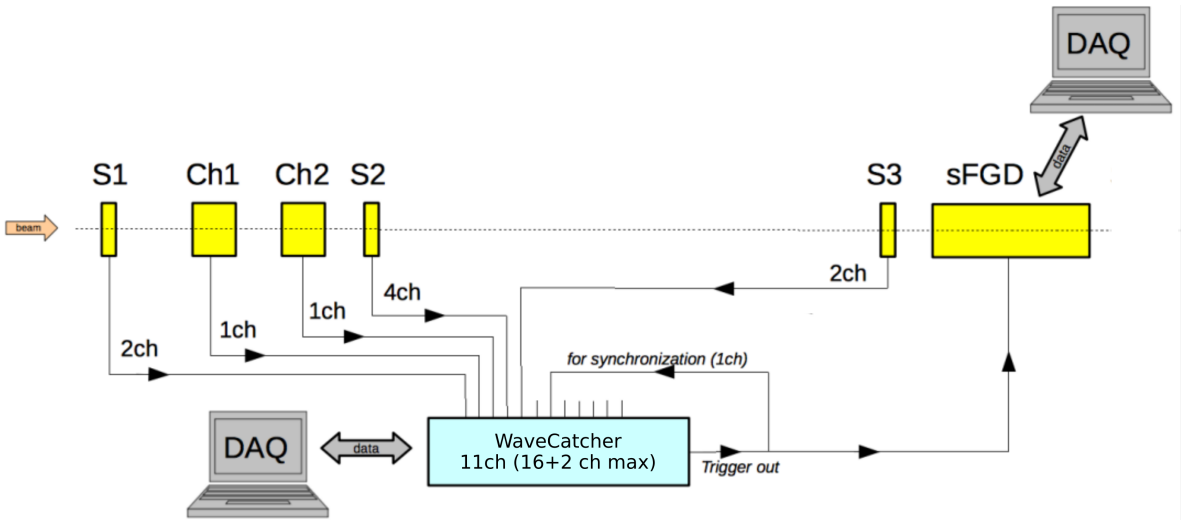

FIG. 8: A schematic of the layout and DAQ for the beam test. The yellow boxes labelled S are beam scintillator counters and the ones labelled Ch are Cherenkov detectors. These are used in the trigger system for the Super-FGD prototype, labelled sFGD in the diagram. PID can be performed with the detectors in the triggering system by using time-of-flight and Cherenkov signals. There are two independent DAQ systems, one based on the WaveCatcher and the other Baby MIND, which is self-triggering. Also shown are the number of channels (ch) from each trigger component [30].

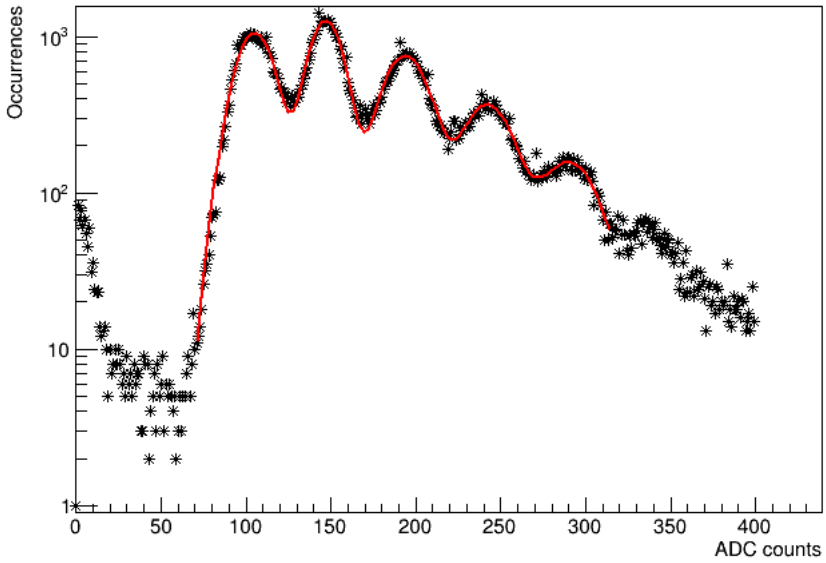

FIG. 9: A histogram of the analogue-to-digital converter (ADC) counts from an MPPC used in the Super-FGD prototype when exposed to low light levels (black markers). The spikes in the data have been fitted with five Gaussian distributions added together (red line) in order to calculate the gain of the MPPC.

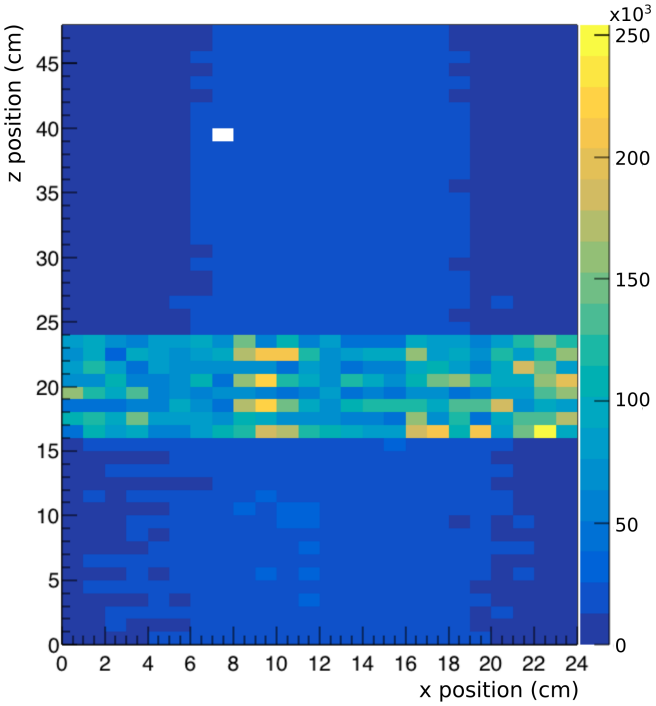

FIG. 10: An event map showing the number of events detected by MPPCs on the horizontal faces of the prototype.

on.

The MPPCs used to read off the signal from the Super-FGD need to be calibrated so that the signal can be converted to the total number of photons detected by the photosensor. One of the calibration requirements is to measure the gain of each MPPC, the gain being the factor by which the initial photoelectron's charge is increased by the MPPC. The gain can be calculated by measuring the gaps between peaks in an MPPC's signal. The signal in Fig. 9 has been fitted with five Gaussian distributions to find the centres of the peaks present in its signal. Measuring the distance between these peaks gives a gain of the MPPC of 46.2 ± 0.5 ADC counts per photoelectron. This measurement needs to be done for all 1728 MPPCs of the Super-FGD detector, which is an ongoing process.

D. Initial Data

The data collected by the Super-FGD prototype during one of the first test beam runs is shown in Fig. 10. The plot shows the number of signals detected by the MPPCs on the top and bottom of the detector. One can see events corresponding to the particle beam by observing the light blue region running through the centre. There is also a bar of noise along the x-axis of the detector. This occurs because the MPPCs here are of a different design to the other regions. In fact, there are three different types of MPPC used on the prototype. The first type correspond to the events shown above the noise bar in the plot. These MPPCs cover the sides and bottom of the detector as well. The region below the bar of noise is another type of MPPC, which explains why the width of the beam seems to be slightly bigger in this region, probably corresponding to cross-talk between scintillator

cubes. These two MPPC types are designed to have low noise levels, whereas the MPPC type found in the noisy region is not. This may look problematic, but the figure only shows the number of events, not the amplitude of events. When data is analysed it will be an easy task to filter out the noise from these MPPCs by rejecting signals with small amplitudes.

The use of several different MPPC types was partly a means to lower the construction costs, as the noisy MPPCs are recycled from the Baby MIND detector, but it also gives an opportunity to test MPPCs with different dynamic ranges and to see which are suitable for the final design.

There is also a noticeable white square in the upper-left region of the event map. This is a faulty MPPC that will be fixed when the prototype is taken out of the magnet for calibration.

Having collected data, it will now be analysed and attempts will be made to reconstruct particle paths. There is no script for an event display written yet, but it is being developed for future use. The plan is to examine data and see if MPPCs that gave a signal at the same point in time can be matched up, which should give the (x, y, z) coordinates of a particle's position.

VII. SOFTWARE CHANGES

In this section, I will outline the changes that have been proposed following discussions from the ND280 software group, some of which are still subject to certain conditions and may change later on.

A. Version Control

CVS has been the version control system (VCS) of ND280 since it was first made. Back then, there were few alternatives and CVS seemed most suited to the task. More recently, however, advances have been made in the world of VCSs with the introduction and popularisation of distributed systems. CVS is a centralised system. The difference between centralised and distributed VCSs is that centralised VCSs require a master repository to which developers commit changes, but distributed VCSs allow developers to "clone" the software and all its metadata to a repository on their own hard drive. There are several advantages to distributed VCSs, including the ability to commit several changes at once, not requiring all developers of the project to see all the changes you make, and not requiring an internet connection for actions other than pulling and pushing data to other repositories.

Given these advantages and many others, the ND280 software will be moved to a Git-based repository. It is most likely, though, that a frozen version of the latest software version at the time of migration will be kept on CMT, as means of a back-up. It's also possible that this CVS version will have any data added to the Git repositories copied over to it, though this is still undecided.

There is also the question of which Git service to use. The choice is between GitHub, a popular VCS that would require a paid subscription to keep the code stored there to be kept private. Alternatively, there is GitLab, a service specifically made with scientific experiments in mind, which requires a private server to be hosted where the repositories can be stored. With this VCS the software will not be viewable by anyone, and specific levels of access can

be given to individuals. There is also the benefit of built-in continuous integration, a feature that makes the process of editing and committing code that much faster.

Following discussions in the software group, it has been decided that the ND280 software will be moved to GitLab rather than GitHub. GitLab offers several features that will be useful for scientific code development. There is also the recent news that GitHub has been purchased by Microsoft, so the future of GitHub and how it will operate is somewhat uncertain, making GitLab a safer and more reliable option. The University of Warsaw, Poland, has offered to host the private servers required to store the software on GitLab.

B. Package Names

The coherent muon to electron transition (COMET) experiment is another experiment situated at J-PARC. It is searching for neutrino-less muon to electron decay. COMET based it's software structure on that of ND280's [31]. In the process of editing the software for their specific use, they updated the package names to make them more consistent and clear. The imminent upgrade could be a good opportunity for ND280's software to follow suit, as there are some arguably confusing names and labelling rules.

A good example of COMET's updated package names is the renaming of the package elecSim to SimDetectorResponse. A developer new to the project would find it hard to discern the role of elecSim in the software (which is to simulate the electronics response of the detector), whereas SimDetectorResponse could not be much clearer. The example also highlights COMET's convention to add a prefix to each package name—such as "Sim" or in other cases "Recon", "Calib" and so on—that indicates where the package will be used in the data flow, i.e. in the simulation, the reconstruction, the calibration or something else. ND280 does this to an extent, but not as consistently, and a suffix is usually used rather than a prefix.

Some other changes made by COMET were the use of capital letters. In ND280, most package names begin with lower-case lettering, but COMET have made each package begin with an upper-case letter (except packages with the "oa" prefix). This is a very basic change but one that arguably makes the names neater and easier to pick out in lists. A change was also made to the lettering of acronyms. For example, the package name "fgdCalib" in ND280 was changed to "CalibFGD". Again, this is a minor change but it makes the name much clearer and avoids confusion between acronyms and words.

From discussions by the ND280 software group, it seems likely that, when the software is migrated to a new VCS, the package names will be updated in a similar manner to the changes made by COMET, although the decision is not yet concrete.

C. CMake and CMT

The final applications of a software package need to be built after the software is edited or downloaded for the first time. From a developer's standpoint the performance of the build-tool is critical as they will have to build the software many times. A user of the software should only need to build the software applications once, so they are more concerned with the ease-of-use of the build tool. The creation and hierarchy properties of ND280's packages have so far been managed by CMT. Many other high energy physics experiments have used CMT with their software, but recently they have been switching to CMake [32]. One

notable example is LHCb, who, until recently, maintained and used CMT before moving to CMake [33].

CMake has an advantage over CMT through it's optimised code. This is especially useful on projects with a large number of packages, such as ND280, where CMT can perform significantly slower than CMake. One caveat, however, is that some features that were present in CMT are absent in CMake. The inheritance of link and compile flags, for example, is included in CMT. This is the process where, if one library (library1) is linked against another (library2), the paths to header files for library2 are included in the compile commands for library1, and all the libraries that were linked to library2 will be included in the link command to library1. In CMake, only the link command feature is included, and not the inherited paths for compile commands. This problem is surmountable because of the CMake language, which allows the construction of custom functions, including the implementation of compile flags.

Overall, the advantages in performance most likely outweigh the work that would be required to include the missing features in CMake. Yet, there is currently still some debate as to whether ND280 should switch to CMake. It has clear advantages over CMT, but, on top of the extra effort of the implementation of features already included in CMT, many of the developers are unfamiliar with CMake, prompting the question of whether the move is worth the effort of learning the language of CMake. Currently, a few developers are attempting to build the ND280 software with CMake, and the results of their efforts will influence the decision of whether to stick with CMT or migrate to CMake.

D. Mix-in Classes

The software of ND280 currently uses ROOT5, but the latest version is ROOT6. It has been decided to update the software to integrate ROOT6, but in doing so a few things must be changed. The implementation of mix-in classes is the most notable issue. Mix-in classes are used in multiple inheritance, where the properties of several classes can be inherited. However, this is not implemented in ROOT6. The problem can be solved by replacing the implementation of the mix-in classes with C macros, but one would also need to alter the user code that accesses the mix-in classes.

To gauge how big a job this would be, I performed a survey on the software to count the number of times mix-in classes are used (they can be identified by the "TM" prefix and "State" suffix in their name). The survey also identified the software packages and files each reference to the mix-in class was made in, but here I will only quote the final count of mix-in classes: five classes inherited a mix-in class and the mix-in classes are directly used in the code 50 times. This is relatively infrequent so the transition to ROOT6 shouldn't be significantly delayed by the reimplementation of these classes.

VIII. (ANTI-)ELECTRON NEUTRINO DETECTION AT ND280

A new Production 7 analysis of RHC beam data from ND280 for ν_e and $\bar{\nu}_e$ charged current interactions producing no pions ($\nu_e/\bar{\nu}_e$ CC-0 π for short) is about to be performed. Some electron neutrino contamination is expected in the muon neutrino beam produced at J-PARC, making it imperative to try to measure this at ND280 to reduce systematic errors when finding the number of muon neutrinos converted to electron neutrinos at SK.

The reference to "Production 7" for the analysis refers to the build of the NEUT software used to generate MC data. The program is continually being improved with updated cross-sections and interaction models, so data is often re-analysed as part of a new production.

Results for the analysis are ongoing. Therefore, in this section, the concepts behind the analysis will be introduced through a description of how cuts can be applied to the data to select ν_e and $\bar{\nu}_e$ events. An outline of the author's upcoming work on the Production 7 analysis will then be given in the final section, along with other future projects.

A. Selection Cuts

The goal of the analysis is to detect electrons (positrons) produced by the weak interaction of a ν_e ($\bar{\nu}_e$) with a nucleus in the fiducial volume of one of the FGD sub-detectors. There will be a large number of background electrons (positrons) present from interaction of other particles, such as pions, which need to be rejected in the analysis. This is made harder by the relatively small number of electrons (positrons) produced in the ν_e ($\bar{\nu}_e$) interactions. Also, accurate PID is needed to distinguish the electrons (positrons) from other particles in the detector such as pions (and, in the case of $\bar{\nu}_e$, protons).

For PID and rejection of background electrons (positrons), a number of cuts are applied to the data. For the Production 6B analysis, there were 12 cuts in total. Only a few of these will be outlined in the interest of conciseness. The full descriptions of the cuts can be found in Technical Note 282 by Christodoulou et al. [34].

Of the 12 cuts applied to the data, several ensure the sampled data had enough information for useful analysis. For example, one cut was the requirement that at least one track must enter a TPC, which is important for PID. This track must produce at least 18 TPC clusters (a cluster is when the charge signal produced by the ionised electrons in the TPC exceeds the required thresholds and quality criteria) if the track enters the ECal, if instead it does not enter the ECal, 36 clusters are required. More detail on the minimum number of TPC clusters can be found in Technical Note 149 [35].

There are also cuts to reduce the background signal. These range from momentum cuts (many background electrons and gammas have momenta below 200 MeV/c) to invariant mass calculations of electron-positron pairs to eliminate gamma backgrounds. PID cuts are also used. For example, selected tracks in events only survive cuts if they have electron, muon and pion pull values (δ_e, δ_μ and δ_π) that lie within certain ranges. A track's pull corresponding to a certain particle is proportional to the difference between the measured ionisation of the track and the expected ionisation produced by the particle. Hence, in the search for ν_e and $\bar{\nu}_e$, one wants a near zero value of δ_e and all other pulls to be far from zero.

Cuts to veto particles originating from outside the detector are also used. Selected tracks must start in the fiducial volume of one of the FGDs and be in coincidence with one of the eight bunches of neutrinos in the beam-line (these bunches are a result of the method of proton acceleration at J-PARC).

The selection of positron tracks from $\bar{\nu}_e$ interactions is more challenging than finding electron tracks from ν_e, as the positrons have the same charge as protons and also have similar energy losses in the TPCs at momenta around 1 GeV [35]. Electrons are easily discerned from protons thanks to the magnetic field in the detector making them curve in opposite directions, but this is not the case for positrons. This means more cuts must be introduced to account for background protons. These cuts look at the ratio between the energy deposited by the particle in the ECal and the momenta of the particles, only letting

tracks with ratios above a certain threshold through to the rest of the analysis.

IX. FUTURE WORK AND CONCLUSIONS

I will now outline how I will progress with my PhD by building upon my initial work and taking advantage of potential research opportunities in the future.

My work on the ND280 software has left many potential avenues of work for me, such as assisting with the transition of the software files from CVS to GitLab. Once the code is transferred it will also need to be maintained. This may include copying anything added to the GitLab repositories to a parallel build of the software kept on CVS, something I could be in charge of. I may also implement a validation system on GitLab that ensures anything uploaded to the software repositories doesn't cause the software to stop functioning.

There is also the switch from CMT to CMake for the software build. This may be done during the transition to GitLab or after. In either case, I will be able to help implement the CMake build with assistance from members of COMET, another J-PARC experiment that is also transitioning their software from CMT to GitLab [31].

I am becoming familiar with the new Super-FGD detector to be installed for the ND280 upgrade thanks to my work on the beam test. This will lead on to me helping with the analysis of the beam test data. From there, I may also become involved with the actual Super-FGD and help to get it ready for installation at ND280.

I will also progress with my work on the Production 7 analysis of ν_e and $\bar{\nu}_e$ at ND280 for the RHC beam data. My future work will involve trying to reproduce the selection plots produced in the Production 6 analysis, then I will move on to using the Production 7 MC data and extracting the ν_e and $\bar{\nu}_e$composition of the beam and the detector's systematic errors by performing fits on the data after selection cuts.

Another potential project for me is the chance to perform an oscillation analysis using the latest data from T2K. This could form quite a large portion of the work I will include in my thesis, so it is important I become more familiar with the techniques and knowledge required for such an analyses.

After joining the T2K group at Imperial College London, I have learnt much about the experiment and gained experience working with software and hardware. Whatever happens over the next few years, there are plenty of exciting options to keep me busy!

---

[1] F. Reines and C. L. Cowan, *The Neutrino*, Nature, **178**, 446–449 (1956).

[2] Y. Fukuda et al., *Evidence for Oscillation of Atmospheric Neutrinos*, Physical Review Letters, **81** (8), 1562–1567 (1998).

[3] A. Suzuki, *Antineutrino science in KamLAND*, The European Physical Journal C, **74** (10) (2014).

[4] F. P. An et al., *Observation of Electron-Antineutrino Disappearance at Daya Bay*, Phys. Rev. Lett., **108**, 171803 (2012).

[5] Y. Abe et al. (Double Chooz Collaboration), *Indication of Reactor $\overline{\nu}_e$ Disappearance in the Double Chooz Experiment*, Phys. Rev. Lett., **108**, 131801 (2012).

[6] K. Abe et al. (T2K Collaboration), *Evidence of electron neutrino appearance in a muon neutrino beam*, Phys. Rev. D, **88**, 032002 (2013).

[7] K. Abe et al. (T2K), *Updated T2K measurements of muon neutrino and antineutrino disappearance using 1.5×10^{21} protons on target*, Phys. Rev., **D96** (1), 011102 (2017), arXiv:1704.06409.

[8] Z. Maki, M. Nakagawa, and S. Sakata, *Remarks on the Unified Model of Elementary Particles*, Progress of Theoretical Physics, **28** (5), 870–880 (1962).

[9] B. Pontecorvo, *Inverse beta processes and nonconservation of lepton charge*, Soviet Physics JETP, **7** (172) (1958).

[10] B. Kayser, *Neutrino physics*, eConf, **C040802**, L004 (2004), arXiv:hep-ph/0506165.

[11] B. Kayser, *B-Meson and Neutrino Oscillation: A Unified Treatment*, AIP Conf. Proc., **1441**, 464 (2011), arXiv:1110.3047.

[12] K. Abe et al., *The T2K experiment*, Nucl. Instrum. Methods Phys. Res. Sect. A, **659** (1), 106–135 (2011).

[13] S. Aoki et al., *The T2K Side Muon Range Detector (SMRD)*, Nucl. Instrum. Methods Phys. Res. Sect. A, **698**, 135–146 (2013).

[14] S. Assylbekov et al., *The T2K ND280 Off-Axis Pi-Zero Detector*, Nucl. Instrum. Meth., **A686**, 48–63 (2012), arXiv:1111.5030.

[15] P. A. Amaudruz et al. (T2K ND280 FGD), *The T2K Fine-Grained Detectors*, Nucl. Instrum. Meth., **A696**, 1–31 (2012), arXiv:1204.3666.

[16] N. Abgrall et al. (T2K ND280 TPC), *Time Projection Chambers for the T2K Near Detectors*, Nucl. Instrum. Meth., **A637**, 25–46 (2011), arXiv:1012.0865.

[17] R. Brun and F. Rademakers, *ROOT — An object oriented data analysis framework*, Nucl. Instrum. Methods Phys. Res. Sect. A, **389** (1-2), 81–86 (1997).

[18] S. Agostinelli et al., *Geant4—a simulation toolkit*, Nucl. Instrum. Methods Phys. Res. Sect. A, **506** (3), 250–303 (2003).

[19] C. Arnault, *CMT: A software configuration management tool*, In *Proceedings, 11th International Conference on Computing in High-Energy and Nuclear Physics (CHEP 2000): Padua, Italy, February 7-11, 2000*, pages 692–695 (2000).

[20] B. Berliner and J. Polk, *Concurrent Version Systems (CVS)* (2001).

[21] S. Ritt, P. Amaudruz, and K. Olchanski, *MIDAS (Maximum Integration Data Acquisition System)* (2001), http://midas.psi.ch.

[22] Y. Hayato, *A neutrino interaction simulation program library NEUT*, Acta Phys. Polon., **B40**, 2477–2489 (2009).

[23] C. Andreopoulos et al., *The GENIE neutrino Monte Carlo generator*, Nucl. Instrum. Methods Phys. Res. Sect. A, **614** (1), 87–104 (2010).

[24] P. Hamacher-Baumann et al., *The T2K-ND280 upgrade proposal*, Technical Report CERN-SPSC-2018-001. SPSC-P-357, CERN, Geneva (2018).

[25] L. Durieu, M. Martini, and A.-S. Muller, *Optics studies for the T9 beam line in the CERN PS East Area secondary beam facility*, In *PACS2001. Proceedings of the 2001 Particle Accelerator Conference (Cat. No.01CH37268)*, IEEE (2001).

[26] T. Brooks, *MNP17* (2015), https://twiki.cern.ch/twiki/bin/view/BL4S/MagneticField.

[27] F. Cadoux, L. Nicola, and E. Noah, *Platform Super-FGD Beam Tests* (2018), https://indico.cern.ch/event/721110/contributions/2964314/attachments/1629976/2597771/Platform_beam_tests_SuperFGD_6April2018.pdf.

[28] M. Antonova et al., *Baby MIND: a magnetized segmented neutrino detector for the WAGASCI experiment*, Journal of Instrumentation, **12** (07), C07028–C07028 (2017).

[29] CAEN, *WaveCatcher Digitisers*, http://www.caen.it/csite/CaenProd.jsp?idmod=857&parent=38.

[30] A. Korzenev, *PID System for the Super-FGD Test-Beam in 2018* (2018), https://indico.cern.ch/event/716235/contributions/2949678/attachments/1623617/2584802/testbeam_sFGD.pdf.

[31] C. Wu, *Search for Muon to Electron Conversion at J-PARC*, Nuclear and Particle Physics Proceedings, **287-288**, 173–176 (2017).

[32] *CMake: Cross-platform Make*, http://www.cmake.org.

[33] M. Clemencic and P. Mato, *A CMake-based build and configuration framework*, Journal of Physics: Conference Series, **396** (5), 052021 (2012).

[34] G. Christodoulou et al., *Selection of electron (anti-)neutrinos at the T2K near detector ND280*, Journal of Physics: Conference Series, **888**, 012218 (2017).

[35] C. Giganti and N. McCauley, *Measurement of the electron neutrino beam component in the ND280 Tracker for 2013 analyses*, TN-149 (2013).